Supporting information

Synergy of Metallic Pt and Oxygen Vacancy Sites over Pt-WO$_{3-x}$ Catalysts for Efficiently Promoting Vanillin Hydrodeoxygenation to Methylcyclohexane

Mengya Sun,[a b] Yanfei Zhang,[a b] Wang Liu,[a b] Xinpeng Zhao,[a b] Hu Luo [a], Gai Miao [a], Zhiqiang Wang [* c], Shenggang Li [* a b d] and Lingzhao Kong [* a b d]

a. CAS Key Laboratory of Low-Carbon Conversion Science and Engineering, Shanghai Advanced Research Institute, Chinese Academy of Sciences, Shanghai 201210, PR China. E-mail: konglz@sari.ac.cn, lisg@sari.ac.cn, wangzhiqiang.ripp@sinopec.com

b. University of Chinese Academy of Sciences, Beijing 100049, PR China.

c. Department of Coal and Syngas Conversion, Sinopec Research Institute of Petroleum Processing, Beijing, 100083, PR China

d. School of Environmental Science and Engineering, Suzhou University of Science and Technology, Suzhou, Jiangsu, 215009, P.R. China.

e. School of Information Science and Technology, Shanghai-Tech University, Shanghai, 200031, PR China

Table of Contents

General Information

Catalyst synthesis and characterization

Chloroplatinic acid hexahydrate, potassium hexachloroplatinate (IV), Potassium hexachloroplatinate (IV), WO_3, Fe_2O_3, Nb_2O_5, vanillin (99.9%), n-hexane (AR), ethanol (AR), cyclohexane (AR), guaiacol (AR), eugenol (99.9%), 4-propyl phenol (AR), 4-ethyl guaiacol (AR) and 4-methoxyphenol (AR) were purchased from Shanghai Macklin Biochemical Co., Ltd.

Pt catalysts were synthesis by wetness impregnation method. The un-calcined (or as received) WO_{3-x} catalyst was detonated as (UC)WO_{3-x}. SiO_2-WO_3 were prepared by Stöber process.[1] A certain amount of deionized water, ethanol and WO_3 was made of liquid suspension, the SiO_2 shell was formation by the sol-gel method. In this method, consecutive hydrolysis and condensation of alkoxysilanes in an aqueous-alcoholic solution in the presence of a base catalyst were involved, using tetraethyl orthosilicate as alkoxysilane and ammonia as the base catalyst. The support samples were impregnated with an aqueous solution of H_2PtCl_6 $6H_2O$ and then dried at 80 °C for 12 h. The as-prepared catalysts were reduced under 5%H_2/Ar flow for 3.0 h at 300 °C. Pt-WO_{3-x}, Pt-K-WO_{3-x}, Pt-Nb_2O_5, Pt-Fe_2O_3, Pt-SiO_2-WO_{3-x} were prepared as the same method and Pt-K-WO_{3-x} was prepared by using K_2PtCl_6 aqueous solution during impregnation processes. Pt-WO_{3-x}(R0), Pt-WO_{3-x}(R1) and Pt-WO_{3-x}(R3) were reduced under 2%H_2/Ar flow for 0 h, 1.0 h and 3.0 h, respectively. Pt-(UC)WO_{3-x} were prepared by using (UC)WO_3 as support.

X-Ray powder diffraction (XRD) was used to analyze the crystal structure of catalysts, running by Rigaku Ultima IVX-Ray diffractometer using Cu Kα radiation in the 2θ range from 5 ° to 80 ° at a scan rate of 4°/min. Thermogravimetry catalysis (TG) was carried out on STA449F3-QMS instrument (NETZSCH). In the experiment, 10 mg of catalyst was weighed and placed into crucible and then purged for 1 h at 150 °C under He and then heated 800 °C under 10%O_2/N_2 to analyze the weight loss of sample. JEM-2100F field emission electron microscope at an operating voltage of 200 kV, equipped with a Gatan 832 CCD camera were used to analyze transmission electron microscopy (TEM), high-resolution transmission electron microscopy (HRTEM) and energy dispersive X-ray spectrum (EDX). X-ray photoelectron spectroscopy (XPS) patterns of samples were analyzed on Thermo Scientific K-Alpha equipped with monochromated Al Kα anode. The binding energies calibration were processing for surface charging by referencing them to the energy of the C1s peak at 284.8 eV. H_2-TPD and NH_3-TPD were all analyzed on Auto Chem. II2920 equipment analyzer (Mircromeritics, USA). The H_2-TPD analysis was recorded from 50 °C to 800 °C at a heating rate of 10 °C/min. NH_3-TPD analysis need same pretreatment for catalysts, and then NH_3 was adsorbed under 50 °C and Ar purge be carried after saturated adsorption. To increase temperature after based line balanced and TCD single were recorded. Brooke A300 electron paramagnetic resonance (EPR) spectrometer was used for obtaining EPR spectra. Raman measurement was performed on a Raman spectrometer (DXR2xi, wavelength of 514 nm).

Reaction tests and products analysis

The activity test was performed in Parr reactor. 10 mL *n*-hexane, 0.06 g Pt-WO$_{3-x}$ and 0.1 g vanillin were putted into autoclave reactor. And then the reactor was purged with H$_2$ five times, pressured to 3.0 MPa by H$_2$ and heated to 230 °C after being sealed. After the reaction, the product was analyzed by GC-FID (Agilent HP-5 column) and GC-MS (Agilent HP-5 column). Own to vanillin can't dissolvent in n-hexane, the reactor and spent catalyst will be washed by ethanol following by analyzing, ensuring vanillin were detected totally. The GC-FID equipped with Agilent HP-5 column (30 m length x 0.25 mm ID x 0.25μm film thickness). The oven temperature as follows: 40 °C (hold 5 min) to 150 °C at 10 °C /min to 300 °C at 20 °C /min. N$_2$ was carrier gas at flow rate of 1 mL/min. The sample was injected with a split ratio of 50: 1. The inlet temperature was 250 °C and detector temperature was 300 °C. Reactant conversion and product selectivity were calculated according to equations:

$$Conversion(\%) = \left(\frac{Mol\ of\ reactant\ consumed}{Mol\ of\ reactant\ added} \right) \times 100\ \%$$

$$Product\ selectivity(\%) = \left(\frac{Mol\ of\ product\ i}{Mol\ of\ reactant\ consumed} / Conversion \right) \times 100\ \%$$
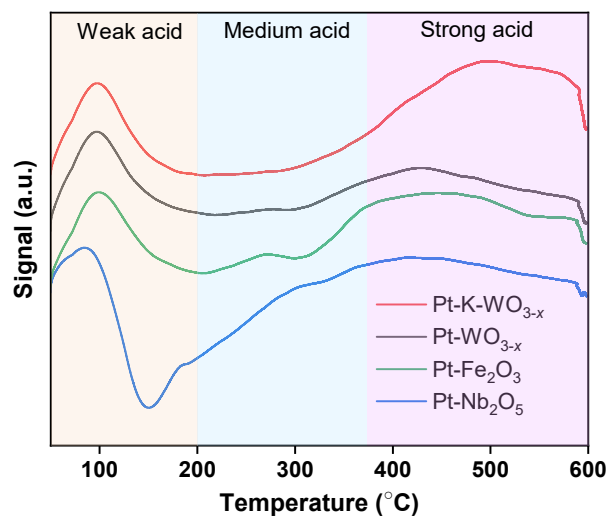
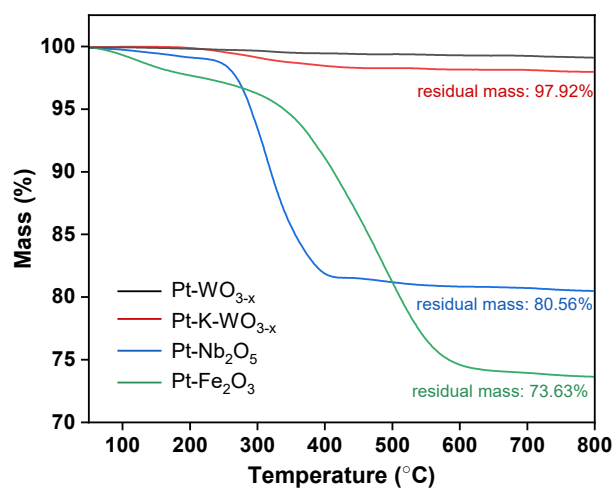**Fig. S1 NH$_3$-TPD spectra of Pt-K-WO$_{3-x}$, Pt-WO$_{3-x}$, Pt-Fe$_2$O$_3$ and Pt-Nb$_2$O$_5$ catalysts**

Fig. S2 TGA thermograms of Pt-WO$_{3-x}$, Pt-K-WO$_{3-x}$, Pt-Fe$_2$O$_3$ and Pt-Nb$_2$O$_5$ spent catalysts
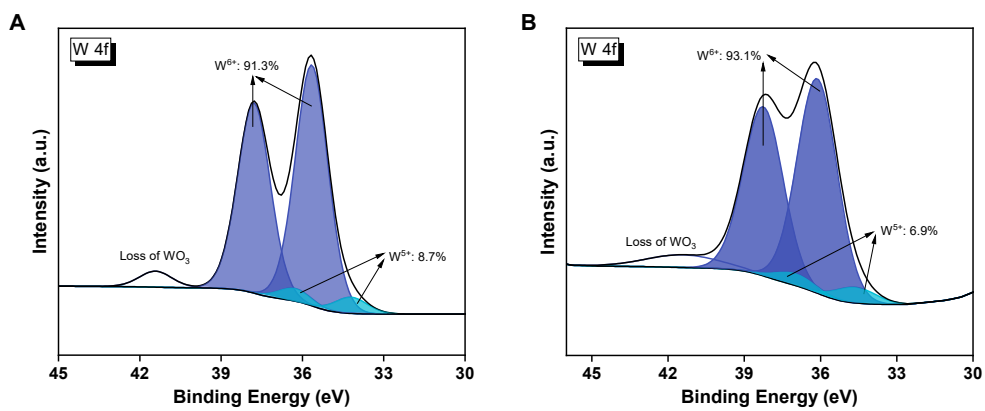
Fig. S3 XPS spectra of W4f over Pt-WO$_{3-x}$ (A) and Pt-SiO$_2$-WO$_{3-x}$ catalysts(B)
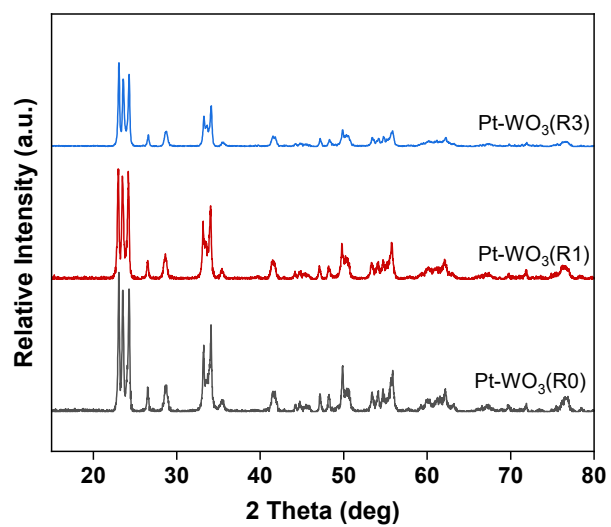
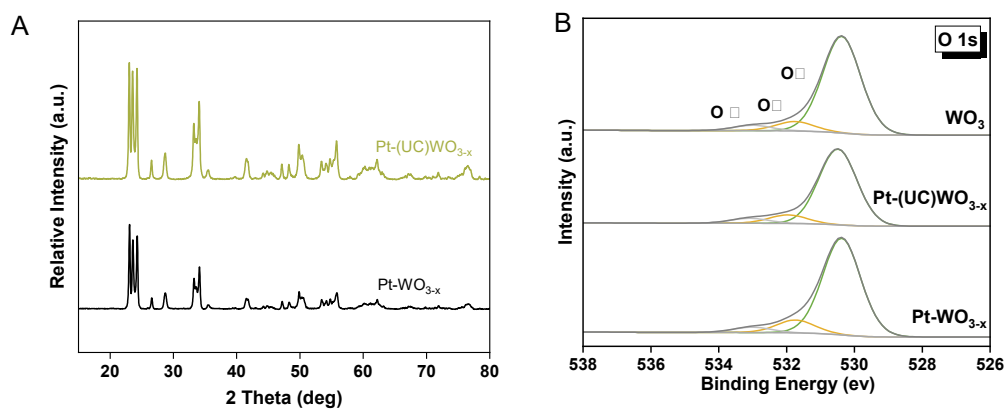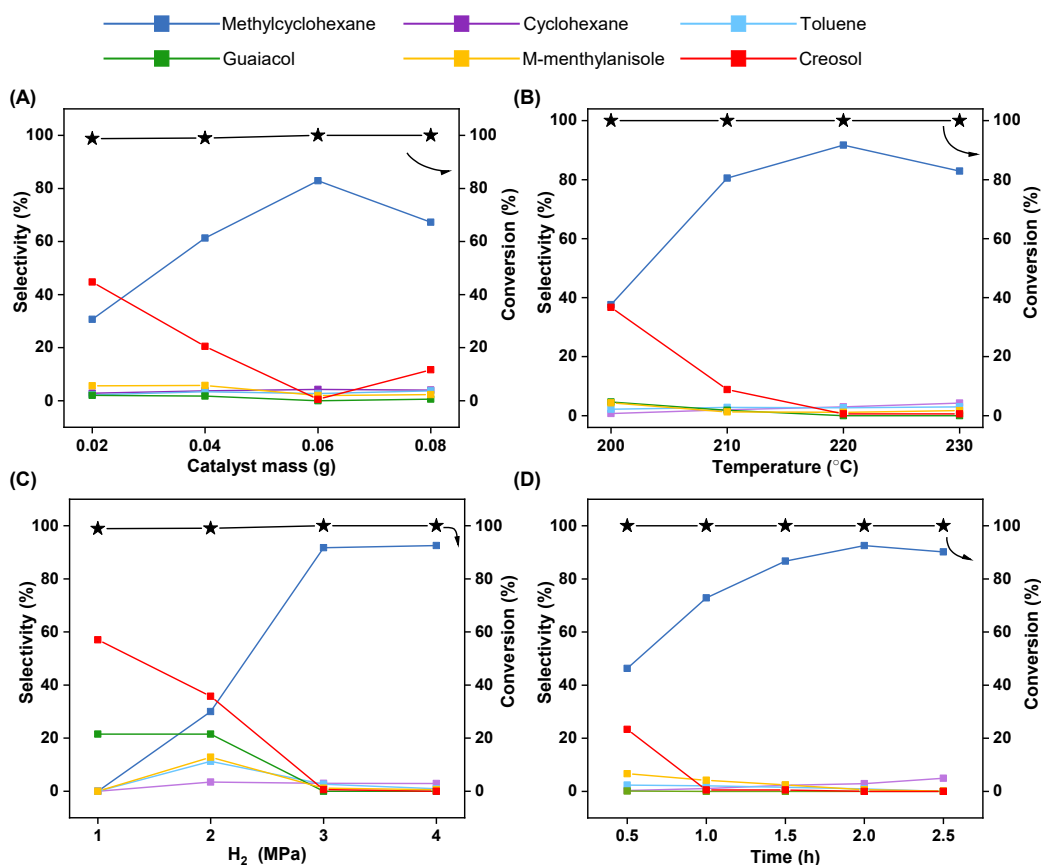**Fig. S4 XRD spectra of Pt-WO$_{3-x}$ catalysts with different reduction time**

Fig. S5 XRD spectra of Pt-(UC)WO$_{3-x}$ and Pt-WO$_{3-x}$ catalysts(A) and the high-resolution O1s XPS spectra(B)

(Reaction condition: (A) Pt-WO$_{3-x}$ catalyst vanillin 0.1 g, 230 °C, 3.0 MPa H$_2$, 10 mL *n*-hexane, 2 h; (B) Pt-WO$_{3-x}$ 0.06 g, catalyst vanillin 0.1 g, 3.0 MPa H$_2$, 10 mL *n*-hexane,2 h; (C) Pt-WO$_{3-x}$ 0.06 g, catalyst vanillin 0.1 g, 220 °C, 10 mL *n*-hexane, 2 h; (D) Pt-WO$_{3-x}$ 0.06 g, catalyst vanillin 0.1 g, 3.0 MPa H$_2$, 10 mL *n*-hexane, 220 °C)

Fig. S6 Effect of catalyst mass, temperature, H$_2$ pressure and reaction time in vanillin HDO over Pt-WO$_{3-x}$ catalysts

The conversion was less than 100% when the catalyst mass was less than or equal to 0.04 g. The H$_2$ pressure will affect the vanillin conversion, which was lower than 100% as the H$_2$ pressure was low than 3.0 MPa. Total conversion of vanillin can be attained under reaction temperature over 200 °C and 3.0 MPa H$_2$ with 0.06 g catalyst and 0.5 h. As the H$_2$ pressure was the main factor for vanillin HDO, MCH selectivity was high to 91.7% when H$_2$ pressure was 3.0 MPa with 0.06 g Pt-WO$_{3-x}$ catalyst and 0.1 g vanillin under 220 °C for 2 h. Under 3.0 MPa H$_2$, the selectivity of MCH and creosol was changed obviously with other different reaction conditions. The other main products selectivity was low than 10% and the change of which was not obvious.
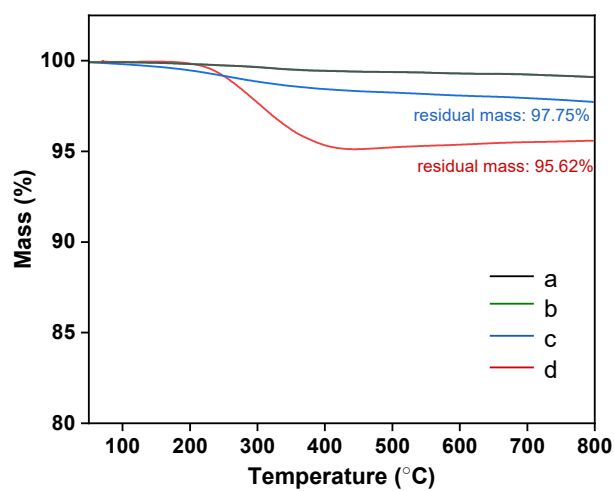
Fig. S7 TGA thermograms of spent Pt-WO$_{3-x}$ catalysts after reaction with different H$_2$ pressure: 1 MPa(a), 2 MPa(b), 3 MPa(c), 4 MPa(d).

The spent Pt-WO$_{3-x}$ catalyst was analyzed by TG. When reaction condition with 1 MPa(a) H$_2$ pressure, the residual mass was 95.62% and TG loss was 4.38%, which owned to carbon deposition of catalyst. There are a few of carbon deposition in the reaction condition of 2 MPa H$_2$ pressure. When H$_2$ pressure increased to 3 MPa, there are almost no carbon deposition in catalysis system.
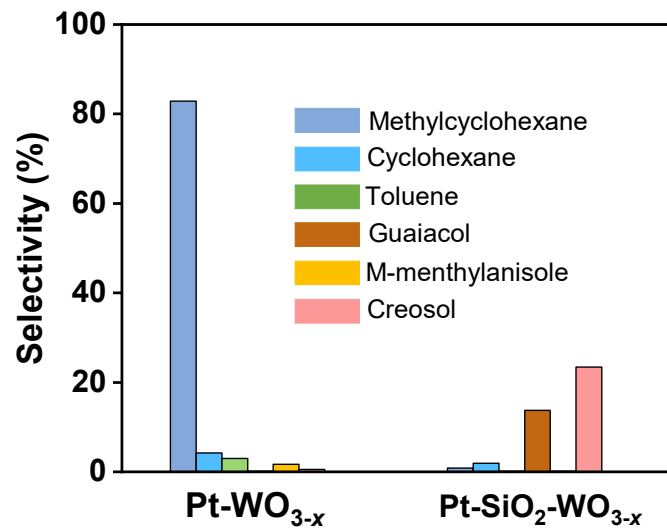
Fig. S8 Vanillin conversion results over Pt-WO$_{3-x}$ and Pt-SiO$_2$-WO$_{3-x}$ catalysts under 230 °C, 3.0 MPa H$_2$, 2 h
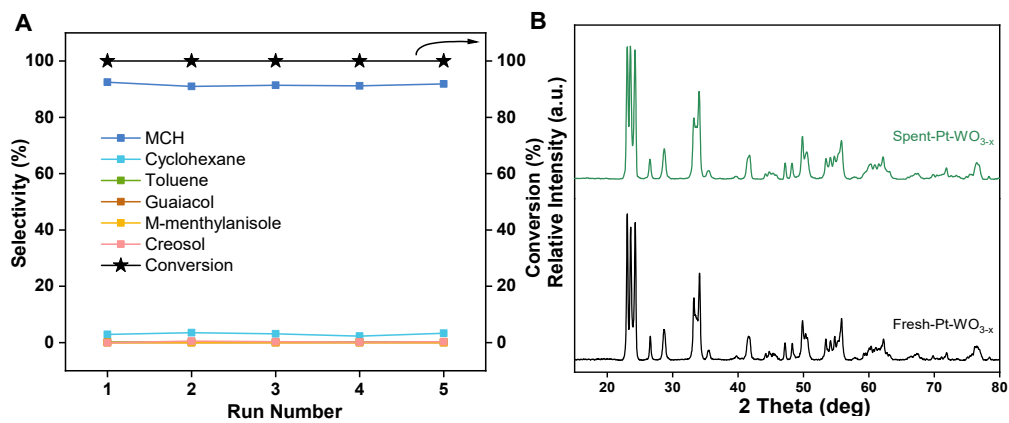
Fig. S9 Recycling tests of Pt-WO$_{3-x}$ for vanillin HDO under 220 °C, 4.0 MPa H$_2$, 2 h; (A) and XRD spectra of fresh-Pt-WO$_{3-x}$ and spent-Pt-WO$_{3-x}$ catalyst (B)

Table S1. The polarity, hydrogen bond donation/ acceptance ability and polarizability of water, ethanol and *n*-hexane

	$E_T(30)$	α	β	π^*
Water	631	117	47	109
Ethanol	519	86	75	54
n-dodecane	311	0	0	05
n-hexane	310	0	0	-04

($E_T(30)$: polarity. **α**: hydrogen bond donation ability. **β**: hydrogen bond acceptance ability. π^*: polarizability) [2]

Table S2. Vanillin conversion results under different solvent over Pt-WO$_{3-x}$ catalysts

Solvent	Conversion/%	Selectivity of main products/%		
		MCH	Creosol	Guaiacol
Water	96.3	5.8	51.1	5.8
Ethanol	99.1	/	92.9	6.1
n-dodecane	/	48.0	/	12.3
n-hexane	>99.9	71.5	0.56	/
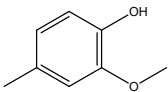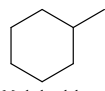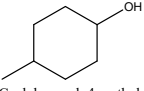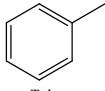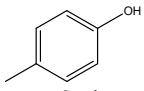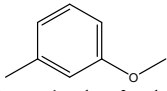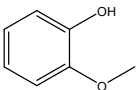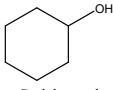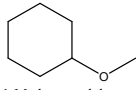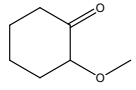
Water and ethanol were protic solvents displaying Lewis basicity and show high polarity[3]. The *n*-hexane and *n*-dodecane are aprotic nonpolar solvents showing no Lewis basicity[2] (Table S2). Although vanillin conversion was more than 95% with each tested solvent with Pt-WO$_{3-x}$, the products selectivity was different (Table S3). Creosol was main product when water and ethanol served as solvent, these polar solvents inhibited the completely HDO of vanillin. It may due to the H-bond between vanillin and the solvent was enhanced, so the adsorption strength of the catalyst and vanillin became weak[4]. Meanwhile, the hydroxyl of solvent and vanillin may form competitive adsorption on the same active site on the catalytic surface, resulting in a decrease in the selectivity of MCH. The nonpolar solvents could supply better environment to obtain MCH. The *n*-dodecane was commonly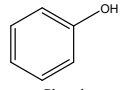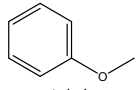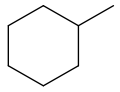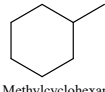 used in the HDO reaction, but here it wasn't better solvent, because there are more guaiacol production for vanillin HDO under *n*-dodecane. Meanwhile, the peaks of creosol and *n*-dodecane appeared in the similar position in GCMS, which make products analysis become difficult. With *n*-hexane solvent, vanillin was efficiently converted and MCH selectivity (71.5%) much higher than that with the other solvents under 230 °C and 3.0 MPa H$_2$. The stability of *n*-hexane was analyzed and there are no detected for MCH when reaction system with *n*-hexane and Pt-WO$_{3-x}$ catalyst. The *n*-hexane own the highest H$_2$ solubility, enabling its adsorption on Pt-WO$_{3-x}$ catalyst surface and further cleavage into reactive species for hydrogenation.[5] This may cause for the higher reactive for completely HDO of vanillin under *n*-hexane solvent.

Table S3. Ratio of each component in W 4f and O 1s for (UC)WO$_3$, WO$_{3-x}$, Pt-(UC)WO$_{3-x}$, Pt-WO$_{3-x}$ catalysts

	Ratio/%				
	W^{6+}	W^{5+}	O I	O II	O III
(UC)WO$_3$	93.7	6.3	87.4	9.9	2.7
WO$_{3-x}$	93.2	6.8	83.6	11.2	4.7
Pt-(UC)WO$_{3-x}$	92.6	7.4	86.5	9.6	3.9
Pt-WO$_{3-x}$	91.3	8.7	81.7	12.8	5.5

In fact, the commercial WO$_3$ was not only with W^{6+}, there are some W^{5+} in the materials by XPS analysis.

Table S4. HDO of some main intermediate products over Pt-WO$_{3-x}$ catalysts

Reactant	Conversion%	Selectivity of products%					
Creosol	77.4	Methylcyclohexane 70.2	Cyclohexanol, 4-methyl- 0.6	Toluene 8.2	p-Cresol 2.4	Benzene, 1-methoxy-3-methyl- 11.4	
Guaiacol	63.7	Cyclohexane 74.3	Cyclohexanol 4.9	1-Methoxycyclohexane 3.0	2-Methoxycyclohexanone 3.4	Phenol 0.6	Anisole 2.4
Methylcyclohexane	/	Methylcyclohexane 100					

(Reaction condition: Pt-WO$_{3-x}$ 0.06 g, vanillin 0.1 g, 220 °C, 3.0 MPa H$_2$, 10 mL n-hexane, 1 h)

In order to analyze the reaction pathway, creosol and guaiacol served as two main kinds of intermediate products were carried out for HDO reaction.

Table S5. Comparison of the results of previously studied catalysts for vanillin HDO completely

Catalysts	T/°C	H$_2$/MPa	t/h	Solvent	MCH yield	Ref.
NiAlOx	280	1.2	4	*n*-hexadecane: *n*-decane=99:1	50%	[6]
Ru/Al$_2$O$_3$	270	4.0	2	Water	16%	[7]
Ru/HZSM-5	170	4.0	4	Water	83.6%	[8]
Ru/HZSM-5	200	5.0	1	Water: octane=2:1	~60%	[9]
Pt-WO$_{3-x}$	220	4.0	2	*n*-hexane	92.5%	This work

References

1. P. Martinez Pancorbo, K. Thummavichai, L. Clark, T. A. Tabish, J. Mansfield, B. Gardner, H. Chang, N. Stone and Y. Zhu, *Adv Funct Mater*, 2019, **29**, 1903549.

2. Y. Marcus, *Chem Soc Rev*, 1993, **22**, 409-416.

3. X. Wang and R. Rinaldi, *ChemSusChem*, 2012, **5**, 1455-1466.

4. F. Héroguel, X. T. Nguyen and J. S. Luterbacher, *ACS Sustain Chem Eng*, 2019, **7**, 16952-16958.

5. Y. B. Huang, A. F. Liu, Q. Zhang, K. M. Li, W. B. Porterfield, L. C. Li and F. Wang, *ACS Sustain Chem Eng*, 2020, **8**, 11477-11490.

6. L. F. Vázquez-Fuentes, M. A. Cortés-Jácome, E. López-Salinas, J. Sánchez-Valente and J. A. Toledo-Antonio, *Catal Today*, 2022, **394-396**, 103-109.

7. I. Yati, A. A. Dwiatmoko, J. S. Yoon, J. W. Choi, D. J. Suh, J. Jae and J. M. Ha, *Appl Catal a-Gen*, 2016, **524**, 243-250.

8. L. Wang, J. Zhang, X. Yi, A. Zheng, F. Deng, C. Chen, Y. Ji, F. Liu, X. Meng and F.-S. Xiao, *ACS Catal*, 2015, **5**, 2727-2734.

9. H. Kim, S. Yang, Y. H. Lim, J.-M. Ha and D. H. Kim, *J Hazard Mater*, 2022, **423**, 126525.